

Sequence-Selective Metal Ion Binding to DNA Oligonucleotides

Nils Åge Frøystein,^{1,*} Jeffery T. Davis,² Brian R. Reid^{2,3} and Einar Sletten¹

¹Department of Chemistry, University of Bergen, Allégt. 41, N-5007 Bergen, Norway and Departments of ²Chemistry and ³Biochemistry, University of Washington, Seattle, WA 98185, USA

Frøystein, N. Å., Davis, J. T., Reid, B. R. and Sletten, E., 1993. Sequence-Selective Metal Ion Binding to DNA Oligonucleotides. – Acta Chem. Scand. 47: 649–657.

Metal ion titrations of several DNA oligonucleotides, 10 dodecamers and one decamer have been monitored by ¹H NMR spectroscopy in order to elucidate metal ion binding patterns. Also, the effects of paramagnetic impurities on resonance linewidths and NOESY cross-peak intensities have been reversed by EDTA back-titration experiments. ¹H 1D NMR spectra were recorded after successive additions of aliquots of different metal salts to oligonucleotide samples. Paramagnetic manganese(II) salts were used in most cases, but a few samples were also titrated with diamagnetic zinc(II). From this study, we conclude that there exists a sequence-selective metal ion binding pattern. The metal ions bind predominantly to 5'-G in the contexts 5'-GG and 5'-GA. The order of preference seems to be GG ≥ GA > GT > > GC. No evidence of metal ion binding to 5'-G in 5'-GC steps or to non-G residues was found. The H6 or H8 resonances on preceding (5'-) bases were affected by the adjacent bound paramagnetic metal ion, but no effect was observed on the protons of the succeeding (3'-) base. The metal binding site in the duplexes is most likely at G-N7, as manifested by the pronounced paramagnetic line broadening or diamagnetic shift of the G-H8 signal. This sequence selectivity may be qualitatively explained by a sequence-dependent variation in the molecular electrostatic potentials of guanine residues (MEPs) along the oligonucleotide chain.

The importance of metal ion interactions with nucleic acids is well established. For instance, metal ions are assumed to participate in the replication, transcription and translation of the genetic code.¹ Metal ions also affect the conformational and structural behaviour of DNA (and RNA).² These conformational perturbations depend both on the type of metal involved and its concentration. Higher concentrations of alkali (or alkaline earth) metals may induce transitions from B-DNA to Z-DNA, and from B-DNA to C-DNA. Alkali and alkaline earth metal ions are not believed to bind to specific sites on a DNA polymer. At high concentrations, at least, these metal ions appear to be electrostatically bound to DNA as counterions in a non-site specific manner, and their behaviour may be explained by polyelectrolyte theory. Interaction with divalent counterions, like Mg(II) and Ca(II), may be important for compact ordered forms of DNA, and interestingly, results from ⁴³Ca NMR³ and ²⁵Mg NMR⁴ studies do indicate that site-specific binding must be considered to explain the observed data. Further support for the existence of a true site-bound calcium is provided in a recent ⁴³Ca NMR study, which included

one of the DNA oligomers studied in this work, d[CGCGAATTCGCG]₂.⁵ Metal ions may be classified according to the hard-soft acid/base scheme, and site-bound alkaline earth metals are likely to bind predominantly to the relatively 'hard' phosphate groups. On the other hand, certain 3d transition metals may bind preferentially to the 'softer' nitrogen sites on the nucleobases. There is no clear borderline for this differential binding to 'hard' and 'soft' sites, however, and early studies showed a remarkable difference in the melting and renaturing properties of native DNA in the presence of different divalent metal ions.⁶

Recently we showed that the transition metal ions Mn(II) and Zn(II) bind selectively to G4-N7 of the DNA oligonucleotide d[CGCGAATTCGCG]₂.⁷ Several studies, especially on platinum binding to DNA, indicate that the metal ions prefer certain base residues in the sequence;⁸ however, no definite rule for this selectivity has been suggested. Also, in the presence of Mg(II) ions, the EcoRV restriction endonuclease cleaves DNA at one particular sequence, GATATC, at least a million times more readily than any other sequence. Substitution of Mg(II) with Mn(II) reduces both EcoRV activity and specificity.⁹ The structural basis for this difference has been related to changes in enzyme-metal bonding proper-

* To whom correspondence should be addressed.

ties, but one must also consider the role of metal ion–nucleic acid interactions in understanding these systems.

Other selective metal ion–nucleic acid interactions have been observed. The chemical nuclease activity of certain phenanthroline copper complexes has been related to the nucleotide on the 5'-side of the site of phosphodiester bond scission.¹⁰ Marzilli and coworkers¹¹ have reported an interesting selectivity pattern for binding of Zn(II) ions to a self-complementary DNA dodecamer. Mercury-induced conformational changes in specific sequences of DNA, monitored by CD spectroscopy, have been shown to alter nuclease activity dramatically.¹² The authors report that polynucleotides with purine-pyrimidine (Pu-Py) sequences undergo Hg(II)-induced CD inversion, while those with Pu-Pu and Py-Pu do not. Other groups have used metalloporphyrins¹³ or inert octahedral complexes¹⁴ as probes for metal binding selectivity to DNA.

The effect of adding paramagnetic metal ions to an aqueous solution of DNA fragments may be monitored by observing the differential line-broadening of specific resonances in the ¹H NMR spectrum.⁷ Correspondingly, the effect of diamagnetic ions is manifested by chemical-shift changes for nuclei close to the metal-ion binding site.^{7,11} Often, in 1D spectra of oligonucleotide molecules containing 10 base pairs or more key ¹H resonances may be severely overlapped, preventing an accurate assessment of the influence of adding metal ions. In these cases 2D-NOESY experiments may provide improved resolution and valuable information. The intensities of NOESY cross-peaks are also reduced by paramagnetic effects from the nearby bound metal ion. Previously we carried out a metal ion titration study on the oligonucleotide duplex, d[CGCGAATTCGCG]₂, which contains the EcoRI recognition sequence -GAATTC-.⁷ In this sequence, most base proton signals are well resolved in the 1D spectrum, enabling one to observe the effect of added metal salts. Substantial line-broadening and chemical shifts were observed for G4-H8 when aliquots of MnCl₂ and ZnCl₂ were added, respectively, while much smaller effects were observed for the other proton resonances in the duplex.

The titration of the EcoRI sequence highlights the sequence dependent metal binding pattern in oligonucleotides. This is manifested through the metal's apparent preference for G4-N7 rather than N7 of residues G2, G10 or G12. The observed preference for guanine residues by 3d transition metals is not surprising, considering the differences in thermodynamic stability of the corresponding nucleoside and nucleotide monomer complexes.² It is also known from platinum–DNA binding studies that guanines generally exhibit greater metal ion affinity than the other base residues, but to date no convincing evidence has been presented showing sequence-selective binding affinity of different guanines along the same oligonucleotide chain. In this paper, we present evidence based on ¹H NMR studies of several oligonucleotides, for the existence of sequence-selective metal ion binding to B-form DNA.

Materials and methods

DNA dodecamers containing the sequences listed in Table 1 were synthesized by using solid-phase phosphite triester techniques as previously described.¹⁵ The synthetic DNA samples were purified by chromatography in distilled water on a 120 cm Sephadex G-25 column and lyophilized to dryness. All the sequences studied were palindromes which readily form duplexes. Thus the annealing step normally used for non-palindrome oligomers was unnecessary.

The samples used for the Mn(II) titrations contained about 50 OD₂₆₀ units of DNA dodecamer, which correspond approximately to 0.55 mM of the duplex. Estimated values for the extinction coefficients¹⁶ will vary due to the different ratios between the numbers of A-T and G-C base pairs and the different base pair orderings. Nevertheless, the variation is small, and all sequences have their extinction coefficients within the range $(1.07-1.23) \times 10^5 \text{ M}^{-1} \text{ cm}$, assuming that all sequences adopt single strand conformations while the measurements are made. The lyophilized samples were dissolved in 0.4 ml of buffer containing 20 mM sodium phosphate (pH 7.0) and 50 mM NaCl. The DNA samples were then repeatedly lyophilized to dryness from D₂O and redissolved in 99.96% D₂O. Finally, the samples were dissolved in 0.4 ml of 99.996% D₂O and transferred to 5 mm NMR tubes. No internal chemical shift standard was used. The Mn(II) solutions were made from a 0.02 M stock solution of MnCl₂ in H₂O (Seattle). Where not stated otherwise, the final concentration of MnCl₂ was 0.02 mM after dilution in D₂O. For the titration carried out in Bergen a 5.1 mM solution of MnCl₂ in H₂O and a 0.051 mM solution of MnCl₂ in D₂O were used. Aliquots of metal salt solution were added directly into the NMR tubes with a micropipette. The samples used for two-dimensional experiments contained from 300 to

Table 1. Paramagnetic broadened and/or chemically shifted guanine H8 resonances (marked in bold) in a series of deoxyoligonucleotide sequences.^a

DNA oligomer sequence	Restriction enzyme recognition sequence
1. 5'-CGCGAATTCGCG*	EcoRI
2. 5'-GCCGATATCGGC*	EcoRV
3. 5'-GCCGTATACGGC*	AccI
4. 5'-GCCAGATCTGGC*	BglII
5. 5'-GAATTTAAATTC	
6. 5'-CGCGTATACGCG*	
7. 5'-GCCGTGCACGGC	
8. 5'-GCCGTTAACGGC	HpaI
9. 5'-GCCTGATCAGGC	BclI
10. 5'-CCAAGCTTGG	
11. 5'-GCCGAATTCGGC	
12. 5'-ATGGGTACCCAT*. ^b	

^aThe line-broadening is induced by paramagnetic impurities. Sequences marked with an asterisk (*) have also been subjected to EDTA treatment and successively titrated with MnCl₂ and/or ZnCl₂ salt. ^bRef. 11.

500 OD₂₆₀ units (ca. 3.3–5.5 mM DNA duplex). The line-broadening effects from paramagnetic impurities in the samples were eliminated by the addition of proper amounts of EDTA, or in some cases the impurities were removed by filtration of the sample through a chelex resin (Biorad). The concentration of the buffer, the pH and the sample volume were identical to those of the 50 OD₂₆₀ samples.

¹H NMR experiments were performed either on a Bruker WM-500 (Seattle) or a Bruker AM-400 WB (Bergen) spectrometer. One-dimensional proton spectra (500 MHz) were typically recorded into 4096 complex points with a 4386 Hz spectral width, a 14 μs pulse width and a recycling delay of 2 s. At 400 MHz the spectra recorded had 4000 Hz spectral widths, and the pulse width was 8.5 μs. During the recycling delay the water resonance was suppressed by a very weak irradiation field. The experiments were made with probehead temperatures in the range 303–309 K.

The typical 2D NOESY^{17,18} spectra (500 MHz) were recorded in the pure-phase absorption mode with quadrature detection using the TPPI method.^{19,20} The data were collected into 1024 complex points in t_2 and 400 or 800 points in t_1 with 32 transients averaged for each t_1 increment. A relaxation delay of 2 s between each transient was used. The spectral width was 4386 Hz and the probehead temperature held at 305 K. In order sequentially to assign the ¹H-resonances in d[GCCGATATCGGC]₂ a single NOESY spectrum was recorded at 400 MHz in the pure-absorption mode with quadrature detection using the hypercomplex acquisition scheme.²¹ 1024 complex points (in t_2) were collected for each of 1024 t_1 increments. 32 transients were averaged for each increment, and a relaxation delay of 2 s was used. The spectral width was 4000 Hz and the temperature was 309 K. In all cases the mixing time was randomly varied ($\pm 10\%$) in order to suppress (actually smear out along F_1 !) zero-quantum J cross peaks.¹⁸ The actual mixing times employed are quoted for each spectrum presented. One DQF-COSY spectrum was acquired at 400 MHz to aid the ¹H resonance assignment of d[GCCGATATCGGC]₂. The DQF-COSY spectrum was acquired in the pure-absorption mode²² with quadrature detection using the TPPI-method.^{19,20} 1024 complex points were collected for each of 1024 t_1 increments. 32 transients were averaged for each increment, and a relaxation delay of 1.7 s was used. The spectral width was 3125 Hz. To avoid rapid-pulsing artifacts and the necessity of using 'dummy' transients, a modified phase cycling scheme due to Derome and Williamson was used.²³ This method has proven extremely effective, and we have used a local modification which manages to include full four-step CYCLOPS,²⁴ axial peak suppression and rapid-pulsing artifact cancellation within 32 transients.²⁵

The 1D NMR data were processed on a Silicon Graphics IRIS-4D computer using the programs FTNMR or FELIX from Hare Research, Inc. The FIDs

were multiplied by an exponential window prior to Fourier transformation. Typically, 2 Hz was added to the linewidths. The spectral baselines were corrected by a third-order polynomial fit. The spectra were referenced to the water resonance set to 4.68 ppm at 305 K and adjusted slightly according to the actual temperature.

The 2D data were zero-filled to 2048 complex points along t_2 , apodized with a 90° phase-shifted and squared sine function, and subjected to a complex Fourier transform. The spectra along F_2 were phase-corrected and baseline-corrected by a third-order polynomial fit. Along t_1 , the data were zero-filled and apodized in an identical manner and finally subjected to a real (for TPPI data) or complex (hypercomplex data) Fourier transform. Prior to Fourier transformation along t_1 , the first increment (F_2 spectrum) was multiplied by 0.5 to avoid the t_1 noise originating from improper scaling in the discrete Fourier transform algorithm.²⁶ This correction is incorporated into FELIX's Fourier transform routines.

Results and discussion

The sequences compared in this work may be divided into two groups according to the type of experiments carried out; duplexes subjected to controlled titration by Mn(II) and/or Zn(II) salts, and duplexes where selective line-broadening was observed both in the 1D ¹H NMR spectra and/or 2D NOESY spectrum, owing to the presence of small amounts of non-specified paramagnetic impurities. To confirm that the line-broadening was caused by traces of paramagnetic metal ions, EDTA was added to these samples in order to chelate the metal ion and eliminate the line-broadening of the affected resonances. These results are summarized in Table 1.

All oligonucleotide syntheses and most of the ¹H resonance assignments were carried out in Seattle. This applies to all oligomers except one, the dodecamer d[GCCGATATCGGC]₂, which was titrated with Mn(II) at 400 MHz (Bergen). Optimal spectral resolution of the aromatic proton resonances in the corresponding one-dimensional spectra was obtained at a temperature of 309 K. The resonance assignments were based on a DQF-COSY spectrum and a 200 ms NOESY spectrum. The sequential assignment followed the standard procedure assuming B-DNA conformation.^{15,27,28} Assignments are presented in Table 2.

Metal ion titration data for the sequence d[CGCGAATTCGCG]₂, which contains the EcoRI recognition site, have already been published.⁷ For this oligomer we observed distinct paramagnetic line-broadening [Mn(II)] and diamagnetic shifts [Zn(II)] which were interpreted in terms of selective metal binding to (or close to) G4-N7. Non-guanine residues were not as affected, except for a significant effect on the H6- and H5-resonances of the residue C3, adjacent to G4 on the 5'-side. In addition, a very slight effect was observed for the overlapping H8-resonances of A5 and A6. The com-

Table 2. ^1H resonance assignments for the DNA dodecamer $\text{d}[\text{GCCGATATCGGC}]_2$ at 309 K.^a

Nucleotide	^1H chemical shifts							
	H2		H1'	H2'	H2''	H3'	H4'	H5'/H5''
	H6/H8	H5/CH ₃						
G1	7.92	5.96	2.58 ^b	2.74	4.81	(4.17) ^{c d}		
C2	7.46	5.36	6.04	2.11	2.46	4.83	(4.22)	
C3	7.37	5.55	5.53	1.97	2.33	4.82	(4.22)	
G4	7.85		5.61	2.68	2.78	4.99	4.33	
A5	8.11	7.69	6.19	2.59	2.87	4.97	4.43	
T6	7.08	1.40	5.66	2.05	2.46	4.84	4.15	
A7	8.15	7.16	6.19	2.56	2.90	4.94	4.38	
T8	7.12	1.25	5.88	1.99	2.41	4.81	(4.17)	
C9	7.36	5.51	5.62	1.92	2.32	4.80	4.07	
G10	7.81		5.58	2.63	2.71	4.95	4.30	
G11	7.71		5.94	2.49	2.70	4.93	4.34	
C12	7.37	5.35	6.14	2.13	2.20	4.47	4.00	

^aThe chemical shifts are referenced to the residual HDO peak, for which the chemical shift has been set to 4.64 ppm. The assignments are based on a DQF-COSY spectrum and a NOESY spectrum with a 200 ms mixing time. ^bThe H2'- and H2''-resonance assignments were resolved by means of the difference in the vicinal couplings between H2'/H3' and H2''/H3'. A C2'-endo sugar conformation, as normally found in B-DNA, was assumed. Under the same assumption these assignments were corroborated by the observed difference in the intensity of the intrasidue H8 (or H6)/H2' and H8 (or H6)/H2'' cross-peaks. Ideally, these intensities should be compared through NOE-buildup curves at shorter mixing times.²⁸ ^cThe chemical-shift values quoted in parentheses are somewhat uncertain owing to severe cross-peak overlap. ^dIt was not possible to resolve the H5' and H5'' resonances utilizing only standard DQF-COSY and NOESY experiments.

plete 3D solution structure of this duplex was previously determined based on NOESY intensities, distance-geometry and NOE back-calculations.²⁹ However, we now show that critical cross-peaks in the NOESY map involving G4-H8 can be drastically affected by paramagnetic impurities. In Fig. 1 a comparison is made between the H6/H8 to H1' region of the original NOESY map (a) and the same region (b) for the oligonucleotide after addition of EDTA. The dramatic differences observed for the G4-H8...G4-H1' and G4-H8...C3-H1' cross-peaks in the two maps obviously introduce large errors in the integrated interproton cross-peak intensities, and consequently may produce structural artifacts. A revised solution structure using a sample with no paramagnetic impurities will be published (Reid *et al.*).

The 1D ^1H NMR titration pattern of the oligonucleotide duplex $\text{d}[\text{GCCGATATCGGC}]_2$ is shown in Fig. 2, and the plot of linewidths versus Mn(II) concentration is shown in Fig. 3. This sequence contains the EcoRV recognition site, -GATATC-. In this case both G4-H8 and G10-H8 are appreciably broadened by Mn(II) ions, while G1-H8 and G11-H8 are relatively unaffected. Furthermore, the paramagnetic relaxation of G10-H8 is approximately twice that of G4-H8. The terminal residue,

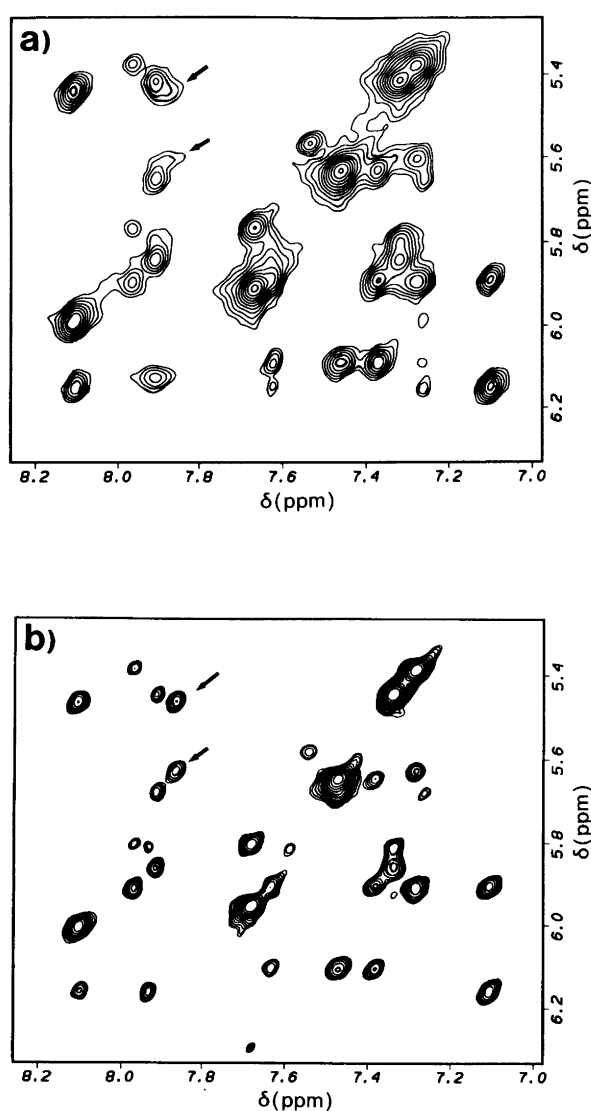


Fig. 1. Contour plots of the H8/H6 versus H1'/H5 region in the 500 MHz NOESY spectra of the dodecamer $\text{d}[\text{CGCGAATTCGCG}]_2$, containing the EcoRI recognition site. The mixing time was 200 ms. The temperature of the probehead was held at 305 K. The spectra shown are (a) the original spectrum without EDTA and (b) with 0.7 mM EDTA added. The intrasidue cross-peak H8-H1' on guanine G4 and interresidue cross-peak between G4-H8 and H1' on cytosine C3 are marked with small arrows (C3-H1' most downfield). Note that, except for the addition of EDTA in (b), the experimental conditions and processing parameters are identical.

G1, appears to be slightly more affected than G11. NOESY maps recorded for this oligonucleotide duplex, before and after EDTA treatment, clearly indicate paramagnetic relaxation of the cross-peaks corresponding to G4-H8 and G10-H8 (Seattle, at 500 MHz; data not shown). In complete agreement with what is found for $\text{d}[\text{CGCGAATTCGCG}]_2$ (*vide supra*), we observe significant paramagnetic broadening of the adjacent C9-H6 resonance on the 5'-side of the most affected

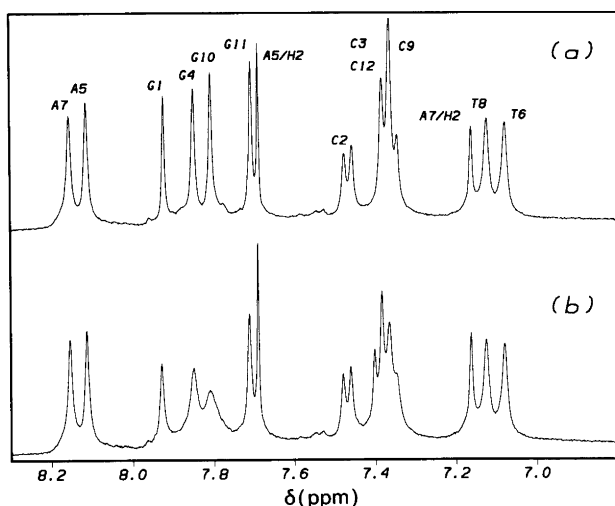


Fig. 2. 400 MHz ^1H NMR spectra, the aromatic region, of the dodecamer $\text{d}[\text{GCCGATATCGGC}]_2$, which contains the EcoRV recognition site. The temperature was 309 K. Shown are (a) the spectrum of the $\text{Mn}(\text{II})$ -free solution and (b) with $50 \mu\text{M}$ MnCl_2 . The H8 and H6 proton resonances for purine and pyrimidine residues are labelled according to their sequential assignment. The chemical shift of the residual HDO resonance is set to 4.64 ppm.

G-residue, G10. From Fig. 2 we note that the overlapping H6 resonances of C3, C9 and C12 change in appearance after metal ion addition. The NOESY spectrum collected at 400 MHz reveals that C9-H6 is the most upfield shifted of these protons (Table 2). This change in appearance may be explained by a paramagnetic broadening of the

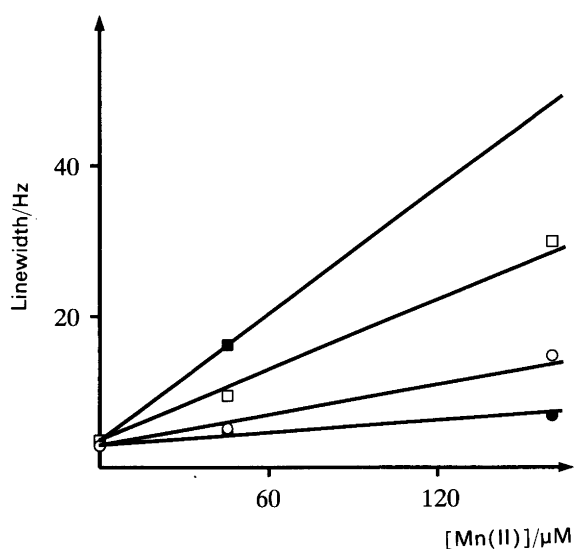


Fig. 3. Paramagnetic linebroadening effects on the guanine H8 proton resonances in $\text{d}[\text{GCCGATATCGGC}]_2$ by the addition of MnCl_2 . The linewidths corresponding to the smallest amount of metal added are taken from the spectrum in Fig. 2b. Filled squares represent H8 of G10, open squares G4, open circles G1 and filled circles G11.

C9-H6 resonance. The addition of higher concentrations of $\text{Mn}(\text{II})$ renders this paramagnetic effect even clearer (spectrum not shown). We observe a slight change in the chemical shift of H6 of C3 or C12 upon addition of metal ion solution. This may be due to small variations in the sample temperature. C9-H6 is the only non-G base proton resonance which is notably perturbed by paramagnetic metal ion titration. By analogy, we should expect that the adjacent residue of G4 on its 5'-side, C3, should display a similar relaxation effect. This is not apparent, however, owing to the spectral overlap of the H6 resonances of C3 and C12. There is also strong overlap of C3-H5 and several H1'-resonances (Table 2). In addition, we may not expect as pronounced an effect at C9-H6, since H8 of G4 is not as severely broadened as that of G10.

The titration of the duplex $\text{d}[\text{GCCGATATCGGC}]_2$ with $\text{Mn}(\text{II})$, which contains the AccI recognition site, causes G10-H8 broadening, leaving the H8 of G1, G4 and G11 unperturbed (data not shown).

Titration with $\text{Mn}(\text{II})$ was also performed on $\text{d}[\text{GCCAGATCTGGC}]_2$. This oligonucleotide contains a fragment, -AGATCT-, which is recognized by the BglII restriction enzyme. The 1D ^1H NMR spectra are shown in Fig. 4, and the H8 linewidths of the G-residues are plotted versus $\text{Mn}(\text{II})$ -concentration in Fig. 5. The lag period in G-H8 line broadening by $\text{Mn}(\text{II})$ is due to a small amount of EDTA initially present in the sample. We find that G5-H8 and G10-H8 are selectively broadened by $\text{Mn}(\text{II})$, whereas the H8 of G1 and G11 are both relatively unaffected. Significant line broadening, although far less

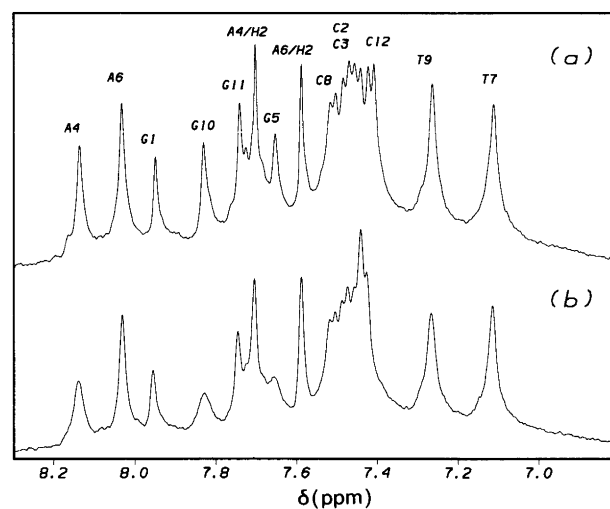


Fig. 4. 500 MHz ^1H NMR spectra, the aromatic region, of the dodecamer $\text{d}[\text{GCCAGATCTGGC}]_2$ which contains the BglII recognition site. The temperature was 303 K. Shown are (a) the spectrum of the $\text{Mn}(\text{II})$ -free solution and (b) with $81 \mu\text{M}$ MnCl_2 . The H8 and H6 proton resonances for the purine and pyrimidine residues are labelled according to their sequential assignment. The chemical shift of the residual HDO resonance is set to 4.70 ppm.

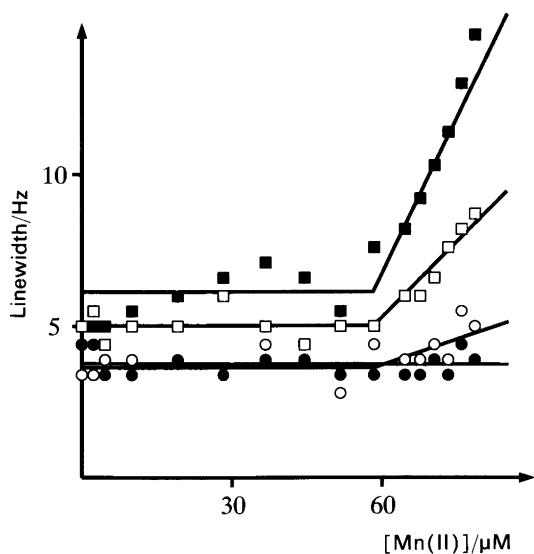


Fig. 5. Paramagnetic linebroadening effects on the guanine H8 proton resonances in $d[\text{GCCAGATCTGGC}]_2$ by the addition of MnCl_2 . The linewidths corresponding to the largest amount of metal added are taken from the spectrum in Fig. 4b. Filled squares represent H8 of G10, open squares G5, open circles G1 and filled circles G11. A $230 \mu\text{M}$ MnCl_2 solution was used for this titration. The large volumes added (0–216 μl) make the concentration scale along the abscissa less convenient than a $[\text{Ligand}]/[\text{Metal}]$ scale.

severe than that found for G5/G10, is also observed for the base protons of the 5'-preceding residues A4-H8 and T9-H6, while broadening effects were not detected for the neighbouring residues on the 3' side. This metal ion selectivity is consistent with our previous observations regarding the dodecamers containing the EcoRI and EcoRV recognition sites (*vide supra*).

Table 1 summarizes the results for 11 different sequences, including those already discussed. Inspection of these data reveals that binding occurs mainly at one or two G-residues in each sequence. The ^1H resonances of the adjacent base residues on the 5'-side of the G-residues which bind metal ions are also broadened, although to a lesser extent than the G-H8 resonances. There is no particular reason to suspect that the nucleotides on the 5'-side of G should be directly involved in the metal ion binding. The broadening of the 5'-residue may be explained as a 'neighbour' effect involving dipolar interaction of these protons and the paramagnetic metal ion bound at the neighbouring G-N7. Other base proton resonances are only marginally affected. It must be stressed, however, that we are discussing only relative broadening effects for each sequence. At higher metal ion concentrations most ^1H resonances undergo varying degrees of broadening.

How do we rationalize these observations? In what base sequence context is the G-residue most affected by paramagnetic metal ion binding? A common feature for several of the sequences is the line-broadening experienced by a G-residue in the context -Py-G-Pu-. However, there is also one example, sequence (4), of a -Pu-G-Pu-

fragment interacting with $\text{Mn}(\text{II})$. Furthermore, in the sequence (5), $d[\text{GAATTTAAATTC}]_2$, G1-H8 is dramatically affected by paramagnetic impurities; this is clearly demonstrated by the restoration of the G1-H8 signal by adding EDTA (Fig. 6). Apparently, a particular lead-in residue on the 5'-side is not a prerequisite for metal ion binding to G-residues. Sequence (5) is the only case with a 5'-G-Pu at the start of the oligonucleotide chain. In all the other sequences studied where the first base is 5'-G, the succeeding residue is a pyrimidine, and in all these cases the G-residue is unperturbed by paramagnetic ions. This leads to the conclusion that 5'-Gs are susceptible to manganese binding whenever the sequence contains 5'-GG or 5'-GA steps. Further support for this proposed rule is found in a paper by Marzilli *et al.*,¹¹ where the sequence $d[\text{ATGGGTACCCAT}]_2$ was titrated with ZnCl_2 [sequence (12) in Table 1]. Here G3-H8 and G4-H8, which both appear in 5'-G-Pu-steps, showed major chemical shifts, while G5-H8 was relatively unperturbed.

One exception to the proposed rule is sequence (6), where G4-H8 in a GT-step is broadened by $\text{Mn}(\text{II})$. However, in this particular duplex there is no 5'-G-Pu-step present to compete with 5'-G-T- for metal ions. A comparison of sequences (3) and (6), where the GT-steps are even flanked by the same residues, shows clearly that H8 of the G in 5'-G-T- is the one most affected by metal ions only as long as there is no competing 5'-G-Pu-. Guanosine has the best donor properties among the nucleoside/nucleotide monomers for metal ion coordination.² As there are no 5'-G-Pu- fragments within the sequence, according to affinity considerations, the available G-residues (if there are any) will be the ones most affected by the kind of added metal ions studied here, $\text{Mn}(\text{II})$ and $\text{Zn}(\text{II})$. Through a careful comparison of sequences (2) and (4) in Table 1 (Figs. 2–5), we suggest that a G-residue in a GG-step is slightly more prone to paramagnetic broadening than in a GA-step. Therefore, the results indicate the following order of metal affinity for G-N7: $\text{GG} \geq \text{GA} > \text{GT} \gg \text{GC}$. However, a more extensive experimental set-up involving several base combinations is needed to determine the affinity pattern quantitatively. Furthermore, stability constants for the DNA/metal ion complexes may be calculated from the paramagnetic contribution to the linewidths. The linewidths are affected by chemical exchange, however, and it will also be necessary to assess the actual dynamical region by measuring linewidths at different temperatures (or fields).³⁰ Alternatively, spin-lattice relaxation rates may be used.³¹ Most of our samples contain EDTA, and samples free of EDTA and paramagnetic impurities should be used in further relaxation studies. The results from the $\text{Zn}(\text{II})$ titration of the dodecamer $d[\text{CGCGAATTCGCG}]_2$ are not suitable for estimating the stability constant, because of unreliable chemical-shift values (i.e. no chemical-shift reference standard was added).⁷

The rule of sequence selectivity presented above is

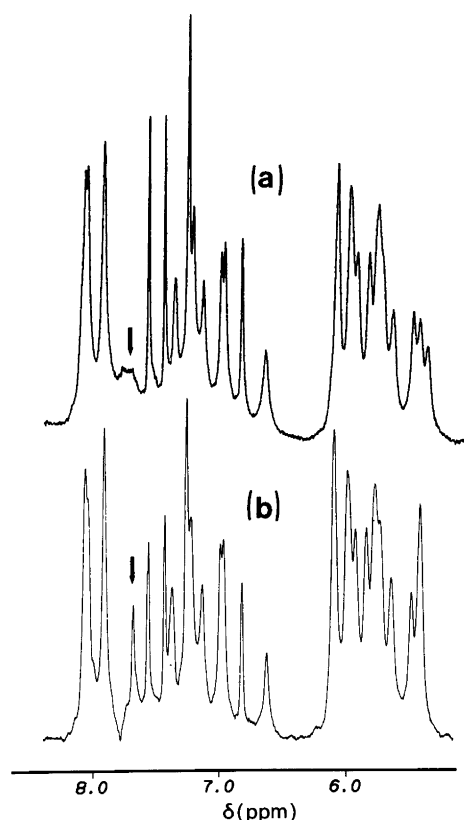


Fig. 6. 500 MHz ^1H NMR spectra at 305 K of the aromatic and H5/H1' region of the dodecamer $[\text{GAATTTAAATTC}]_2$, (a) without EDTA and (b) with 0.4 mM EDTA. The small arrows mark the H8 resonance of the guanine G1. The chemical shift of the residual HDO resonance is arbitrarily set to 4.68 ppm.

based on Mn(II) and Zn(II) titration and EDTA back-titration of paramagnetically contaminated samples. At present we have no clear understanding of the mechanism which governs this general metal-DNA interaction. Several models have been proposed for binding of metal ions to DNA, including inter- or intra-strand cross-linking of adjacent bases, chelate complexes involving N7 and a phosphate group, or metal sandwich-type intercalation. All these models require a relatively large distortion of the helix geometry in order to accommodate the metal ions. For diamagnetic complexes in near-stoichiometric M^{2+}/DNA ratios, induced conformational distortion of the duplex should, in principle, be easily detected in 2D NOESY maps, J -coupling patterns or ^{31}P spectra. However, Marzilli *et al.*¹¹ (*vide supra*) conclude that no major distortion of a DNA duplex by added metal ion $[\text{Zn}(\text{II})]$ is evident from the NMR data.

The predominant binding pattern observed in numerous studies of metal complexes of guanine mononucleotides and analogs³² involves monodentate binding to N7 stabilized by a strong intra-complex hydrogen bond between the metal ion's coordination sphere and the carbonyl substituent O6. Based on the present observations we suggest that Mn(II) and Zn(II) bind G-N7 directly in DNA oligomers as well. This is not unreasonable considering

the relatively wide major groove of B-DNA, which is the expected conformation for the oligonucleotides under the conditions studied. In addition, the observed 5'-neighbour effect is easily incorporated into this structural model. We are comparing the same type of nucleotide (G) at different positions in a given DNA sequence in the presence of the same metal ion. The exposed guanines at the 5'- or 3'-ends of the sequences are not affected by paramagnetic metal, except for one case where the G1 is followed by adenine (Table 1). This is in agreement with the proposed 5'-G-Pu rule. Thus, steric factors alone do not seem capable of explaining the specific paramagnetic relaxation observed. We suggest that the magnitude of the partial negative charge on the potential binding sites of the nucleobases themselves is a major factor which determines the preferred metal ion binding site and coordination geometry.

Theoretical calculations of the molecular electrostatic potentials (MEPs) along the double helix show marked sequence-dependent variations.³³ $\Delta(\text{MEP})$ was calculated for N7 of 5'-G in series of triple bases:³³ GGR (-14.9), GGY (-12.8), GAR (-12.9) and GAY (-8.0), where R = purine and Y = pyrimidine. The corresponding values for GTR, GTY, GCR and GCY were -7.4, -7.2, -4.1 and -1.5, respectively. Clearly the magnitude of $\Delta(\text{MEP})$ on N7 of 5'-G residues in GG- and GA-steps compared to GC- and GT-steps suggests that the former are more susceptible to metal binding. The preference for metal ion binding to 5'-G in the context 5'-GG or 5'-GA may be directly related to a redistribution of charge between the base residues so as to favour monodentate G-N7 binding. The presently postulated GG/GA rule is only expected to account for the major trend in metal ion binding selectivity. The flanking residues, as expected, modify the MEP to a certain degree; e.g. 5'-CGG (sequence 2 of Table 1) may be more reactive than 5'-TGG (sequence 4 of Table 1). The calculations are based on regular B-DNA geometry. More realistic theoretical MEP values may be obtained by using experimentally determined coordinates for the oligonucleotides either based on X-ray or NMR data. Fluctuation in the nucleophilicity of G-N7 sites as a consequence of subtle sequence-dependent conformational changes that alter base stacking could account for the metal binding patterns. At present, our paramagnetic line-broadening and diamagnetic shift studies have enabled us to detect only the major trends in the order of affinity between different sites.

The selectivity of alkylation reactions, where positively charged groups attack specific G-residues at N7, may be analogous to the observed sequence selectivity for metal cation-DNA interaction.³⁴ The reported six- to eight-fold variation between methylation intensities at different guanines in a DNA fragment suggests the possibility of sequence-dependent variations in G-N7 nucleophilicity. Indeed, for small alkylating groups there seems to be a positive correlation between reactivity at certain sites and MEP.³⁵ However, in addition to the influence from

neighbouring bases, global factors are also reported to be of importance.³⁴

Preliminary results indicate that the sequence selectivity is dependent on the identity of the metal ions. While Mn(II) and Zn(II) ions are found to bind in a similar fashion to G-residues,⁷ Co(II) ions also seem to interact selectively with certain A-residues as well as G-residues (unpublished results), and Hg(II) ions when added to the EcoRI duplex bind to thymidine residues (unpublished results). Experiments are in progress in our laboratories to elucidate this metal ion dependent sequence selectivity further.

CD studies³⁶ on metal-induced conformational changes in DNA polynucleotides show large variation in the bonding patterns for different metal ions. For example, ions such as cadmium(II) induce a B to Z transition in poly d(G-C), whereas copper(II) causes a B to A transition. By far the largest number of metal-DNA studies involve platinum ions, reflecting the importance of this metal in antitumor drug therapy. In one of these studies,⁸ where platination of DNA from salmon sperm was carried out, followed by enzymatic digestion, chromatographic separation of different fractions showed a predominance for Pt-GpG species (65%), a somewhat smaller portion of Pt-ApG (25%) and minor fractions of Pt-N monomers. No Pt-GpA species were observed. This result does not quite agree with our postulated rule, which predicts metal binding to GG and GA steps but not to AG steps. This might indicate that divalent platinum in the cis-platin drug has a different interaction pattern than the metal ions we have studied to date. One interesting observation in this context is the observed difference between Pt(II) and Pt(IV) compounds, the latter being far more inert and unable to react with DNA under ambient conditions.⁸ The Pt(IV) complex has to be reduced to the square-planar Pt(II) compound to exhibit antitumor activity. Differences in coordination geometry between the elements included in this study [Mn(II) and Zn(II)] and Pt(II) may also help explain the apparent shift in affinity from a GA to a AG step.

Conclusion

We have demonstrated the sequence-selective binding of some divalent 3d transition metal ions to short DNA oligomers. Certain guanines appear to be the preferred targets for these metal ions. Moreover, we have addressed the question of how the metal selects its preferred N7 binding site among several such sites on different guanines along the DNA duplex. Among the sequences, which contain from one to five different guanines, only one or two of the corresponding H8 resonances are significantly broadened by Mn(II) ions at very low concentrations or diamagnetically shifted, in the case of added Zn(II). The only other resonances which are affected are the H8 or H6 resonances of the neighbouring nucleotides on the 5'-side of the affected guanines.

A rule is proposed for the preferential binding of

Mn(II) and Zn(II), where N7 on guanine in a 5'-G-purine step is presumed to be the primary site for metal ion coordination. Inspection of the data suggests the following order of preference: $GG \geq GA > GT > > GC$. The observed order of metal ion binding in these oligonucleotide duplexes can be correlated with the molecular electrostatic potential (MEP) of the G-residues in the DNA helices.

Acknowledgments. N. Å. F. gratefully acknowledges the Royal Norwegian Council for Scientific and Industrial Research (NTNF) and the Norwegian Council for Science and the Humanities (NAVF) for fellowships. E. S. gratefully acknowledges a travel grant from the Norwegian Council for Science and the Humanities (NAVF). J. T. D. and B. R. R. gratefully acknowledge support from National Institute of Health (NIH) grants F32 GM14340-01 and GM-32681.

References

1. Eichhorn, G. L. and Marzilli, L. G. *Advances in Inorganic Biochemistry*. Elsevier/North-Holland, New York 1981, Vol. 3.
2. Eichhorn, G. L. In: Eichhorn, G. L., Ed., *Inorganic Biochemistry*, Elsevier, Amsterdam 1973, Vol. 2, Chap. 33-34.
3. Braunlin, W. H., Drakenberg, T. and Nordenskiöld, L. *Biopolymers* 26 (1987) 1047.
4. Rose, D. M., Polnaszek, C. F. and Bryant, R. G. *Biopolymers* 21 (1982) 653.
5. Braunlin, W. H., Nordenskiöld, L. and Drakenberg, T. *Biopolymers* 28 (1989) 1339.
6. Eichhorn, G. L. and Shin, Y. A. *J. Am. Chem. Soc.* 90 (1968) 7323.
7. Frøystein, N. Å. and Sletten, E. *Acta Chem. Scand.* 45 (1991) 219.
8. Fichtinger-Schepman, A. M. J., van der Veer, J. L., den Hartog, J. H. J., Lohman, P. H. M. and Reedijk, J. *Biochemistry* 24 (1985) 707.
9. Vermote, C. L. M. and Halford, S. E. *Biochemistry* 31 (1992) 6082.
10. Yoon, C., Kuwabara, M. D., Spassky, A. and Sigman, D. S. *Biochemistry* 29, (1990) 2116.
11. Jia, X., Zon, G. and Marzilli, L. G. *Inorg. Chem.* 30 (1991) 228.
12. Gruenwedel, D. W. and Cruikshank, M. K. *Biochemistry* 29 (1990) 2110.
13. Strickland, J. A., Marzilli, L. G., Wilson, W. D. and Zon, G. *Inorg. Chem.* 28 (1989) 4191.
14. Pyle, A. M. and Barton, J. K. In: Lippard, S. J., Ed., *Progress in Inorganic Chemistry: Bioinorganic Chemistry*, Wiley, New York 1990, Vol. 38, pp. 413-475.
15. Hare, D. R., Wemmer, D. E., Chou, S.-H., Drobny, G., Reid, B. R. *J. Mol. Biol.* 171 (1983) 319.
16. Borer, P. N. In: Fasman, G. D., Ed., *Handbook of Biochemistry and Molecular Biology*, 3rd ed., CRC, Cleveland OH 1975, p. 589.
17. Jeener, J., Meier, B. H., Bachmann, P. and Ernst, R. R. *J. Chem. Phys.* 71 (1979) 4546.
18. Macura, S., Huang, Y., Suter, D. and Ernst, R. R. *J. Magn. Reson.* 43 (1981) 259.
19. Redfield, A. G. and Kunz, S. D. *J. Magn. Reson.* 19 (1975) 250.
20. Bodenhausen, G., Kogler, H. and Ernst, R. R. *J. Magn. Reson.* 58 (1984) 370.

21. States, D. J., Haberkorn, R. A. and Ruben, D. J. *J. Magn. Reson.* **48** (1982) 286.
22. Rance, M., Sørensen, O. W., Bodenhausen, G., Wagner, G., Ernst, R. R. and Wüthrich, K. *Biochem. Biophys. Res. Commun.* **117** (1983) 479.
23. Derome, A. E. and Williamson, M. P. *J. Magn. Reson.* **88** (1990) 177.
24. Hoult, D. I. and Richards, R. E. *Proc. R. Soc. London, Ser. A* **344** (1975) 311.
25. Frøystein, N. Å. *Unpublished results.*
26. Otting, G., Widmer, H., Wagner, G. and Wüthrich, K. *J. Magn. Reson.* **66** (1986) 187.
27. Scheek, R. M., Russo, N., Boelens, R., Kaptein, R. and van Boom, J. H. *J. Am. Chem. Soc.* **105** (1983) 2914.
28. Scheek, R. M., Boelens, R., Russo, N., van Boom, J. H. and Kaptein, R. *Biochemistry* **23** (1984) 1371.
29. Nerdal, W., Hare, D. R., Reid, B. R. *Biochemistry* **28** (1989) 10008.
30. Swift, T. J. and Connick, R. E. *J. Chem. Phys.* **37** (1962) 307.
31. Luz, Z. and Meiboom, S. *J. Chem. Phys.* **40** (1964) 2686.
32. Sletten, E. In: Pullman, B. and Goldblume, N., Eds. *Metal-Ligand Interaction in Organic Chemistry and Biochemistry*, Part 1, D. Reidel, Dordrecht 1977, pp. 53-64.
33. Pullman, A. and Pullman, B. *Q. Rev. Biophys.* **14** (1981) 289.
34. Wurdeman, R. L., Church, K. M. and Gold, B. *J. Am. Chem. Soc.* **111** (1989) 6408.
35. Kohn, K. W., Hartley, J. A. and Mattes, W. B. *Nucl. Acid Res.* **15** (1987) 10531.
36. Narasimhan, V. and Bryan, A. M. *Inorg. Chim. Acta* **91** (1984) L39.

Received September 8, 1992.